

Biased evolutionary inferences from bulk tumor samples

*J.M. Alves, T. Prieto, D. Posada**

Department of Biochemistry, Genetics and Immunology and Biomedical Research Center (CINBIO), University of Vigo, Spain. Galicia Sur Health Research Institute, Vigo, Spain.

* corresponding author

Keywords: Intratumor genetic heterogeneity, somatic evolution, phylogenetic inference, bulk sequencing

1 **ABSTRACT**

2 It is generally agreed that tumors are composed of multiple cell clones defined by
3 different somatic mutations. Characterizing the evolutionary mechanisms driving
4 this intratumor genetic heterogeneity (ITH) is crucial to improve both cancer
5 diagnosis and therapeutic strategies. For that purpose, recent ITH studies have
6 focused on qualitative comparisons of mutational profiles derived from bulk
7 sequencing of multiple tumor samples extracted from the same patient. Here, we
8 show some examples where the naive use of bulk data in multiregional studies
9 may lead to erroneous inferences of the evolutionary trajectories that underlie
10 tumor progression, including biased timing of somatic mutations, spurious parallel
11 mutation events, and/or incorrect chronological ordering of metastatic events. In
12 addition, we analyze three real datasets to highlight how the use of bulk
13 mutational profiles instead of inferred clones can lead to different conclusions
14 about mutational recurrence and population structure.

15

16

17

18

19

20

21

22

23

24

25

26

27

28

29

30

31

32

33

34

35 INTRODUCTION

36 Over the past decade, global sequencing efforts of cancer genomes have
37 revealed that genetic intratumor heterogeneity (ITH) represents a common
38 feature of many cancer types¹, arising from the progressive accumulation of
39 somatic mutations within malignant cells during cancer evolution². As a result,
40 single tumors typically comprise multiple genetically distinct subpopulations of
41 cells (i.e., clones), which may vary with regards to growth, metastatic potential,
42 and therapeutic resistance^{2,3}. With the increasingly obvious clinical implications
43 of ITH⁴, a great deal of attention is currently being directed towards exploring the
44 complex patterns of clonal heterogeneity under an evolutionary framework, in
45 order to resolve the genetic history underlying cancer progression⁵⁻⁷ and gain a
46 wider understanding of the evolutionary mechanisms driving tumor
47 diversification⁸⁻¹¹. Indeed, following the pioneer work by Gerlinger *et al.*¹²,
48 reporting a high degree of variation in the genetic composition of primary tumors
49 and metastases as a consequence of divergent clonal evolution, a number of
50 studies have focused on the spatial and temporal dynamics of tumorigenesis,
51 taking advantage of next-generation sequencing (NGS) data obtained from bulk
52 tissue samples extracted from multiple tumor regions within a single patient^{10,13-}
53 ¹⁶.

54
55 However, although a variety of statistical algorithms exist to infer the clonal
56 composition of tumors from bulk NGS data (see Beerenwinkel *et al.*¹⁷ for an
57 exhaustive review), most multiregional sequencing studies still analyze the
58 spatial patterns of clonal diversity by directly comparing mutational profiles
59 (absence/presence of mutations) across samples. For example, making use of
60 whole-exome bulk sequencing data initially derived from 23 evenly distributed
61 samples in a cross-section of a hepatocellular carcinoma, Ling *et al.*¹⁸ identified
62 a set of 35 somatic single-nucleotide variants (SNVs) that were subsequently
63 used to genotype approximately 300 samples of the same tumor. Ancestral
64 relationships among the sampled regions were inferred from their mutational
65 profiles, and used to delineate clonal boundaries and reconstruct clonal
66 genealogies. Consistent with previous findings¹⁰, the authors observed extensive
67 genetic diversity between all regional samples, pointing to a limited role of
68 selection, with patterns of genetic diversity suggesting the appearance of new

69 subclones on the peripheries of tumors which tend to radiate outwards. Similarly,
70 Zhao *et al.*¹⁹ applied a series of phylogenetic methods to whole-exome
71 sequencing data derived from 40 cancer patients to address the origin of
72 metastases. By analyzing the mutational profiles of primary tumors and
73 associated metastases, the authors concluded that metastatic lineages often
74 evolved non-linearly from the primary tissue, suggesting that metastases may
75 originate stochastically from distinct clonal lineages within the primary tumor of a
76 given patient. In order to trace the timing of such metastatic events, the authors
77 further transformed the inferred regional trees into patient-specific chronograms,
78 calibrated a molecular clock based on different clinical parameters, and
79 suggested that most metastatic lineages appeared to differentiate at very early
80 stages of cancer progression, usually prior to clinical detection.

81

82 Importantly, at the heart of these studies is the implicit assumption that tumor
83 clones present in a tissue sample can be meaningfully summarised as the
84 collection of mutations observed in that sample (i.e., the mutational profile) –or
85 that only a single or dominant clone exists per sample that carries all mutations–
86 , and that reliable evolutionary relationships can be inferred from such
87 information. However, given the high levels of ITH expected in most tumors, this
88 assumption is not justified and can lead to biased inferences regarding the
89 evolutionary history of a tumor.

90

91

92 **IMPLICATIONS OF MUTATIONAL PROFILES FOR EVOLUTIONARY** 93 **INFERENCE**

94

95 *Mutational histories*

96 Since most tumors consist of a genetically heterogeneous population of cells,
97 mutational profiles of bulk tumor samples essentially reflect the set of somatic
98 mutations present in a detectable fraction of the cells sampled, but not
99 immediately the collection of clones present. The fundamental reason for this is
100 that, in the absence of single-cell information, the precise combination of
101 mutations that occur in any given clone is unknown, and a set of n mutations can
102 represent 1, 2 or even n clones. In the presence of ITH, multiple clones are

103 expected per bulk sample, hence the observed mutational profile might easily
104 correspond to a “composite clone” that never existed. Consequently, the use of
105 mutational profiles as units for evolutionary analysis can have important
106 implications.

107

108 To illustrate this idea, consider the cancer patient shown in **Fig. 1A**, whose
109 primary tumor harbors three genetically distinct cell clones A-C resulting from the
110 accumulation of five somatic mutations. The three clones share some mutations
111 (“true clonal sequences”) that reflect their common history from a common
112 ancestor (“true clonal phylogenetic tree”). For simplicity, we assume that the
113 tumor does not contain healthy cells (i.e., no contamination). **Fig. 1B** depicts a
114 hypothetical multiregional sequencing study, where three spatially separated
115 regions from the primary tumor have been sampled and sequenced. While the
116 sampling scheme shows that all three clones have been captured, the proportion
117 of each cell clone per sample varies, with sample I consisting entirely of cells
118 belonging to clone A, sample II being composed of cells from clones B (80%) and
119 C (20%), and sample III carrying cells from clones A (30%) and C (70%).
120 Accordingly, only the mutational profile for sample I corresponds to a true clonal
121 sequence (clone A), while the profiles obtained for the other two samples
122 represent a composite of clones BC and AC, respectively. If we now build a
123 maximum parsimony (MP) tree using these composite clones (see Gerlinger *et*
124 *al.*¹²; Gerlinger *et al.*¹⁴; Hao *et al.*¹⁶; Ling *et al.*¹⁸), we would wrongly infer that
125 mutations 1, 2 and 3 occurred in the most recent common ancestor (MRCA) of
126 these samples, and that mutation 5 occurred before mutation 4. Importantly,
127 these problems can be avoided if one realizes that the history of the samples is
128 often not the same as the history of the clones. Indeed, in recent years multiple
129 algorithms have been developed for the identification of clones from bulk tumor
130 samples¹⁷, usually by clustering mutations with similar variant allele frequency
131 (VAF) into single clones. In this example, the clustering algorithm implemented
132 in Clomial²⁰ perfectly identifies the true clones. A MP tree of these clonal
133 sequences accurately recovers the true clonal history and the right order of
134 mutations (**Fig. 1C, Supplementary Note**).

135

136 **Fig. 2** illustrates another example involving the same hypothetical cancer patient
137 (**Fig. 2A**), but for which a distinct set of regional samples was obtained (**Fig. 2B**).
138 In this case, the use of mutational profiles results in a phylogenetic tree in which
139 mutation 5 spuriously appears to have occurred twice, independently in sample
140 II and III. Again, the use of a clustering algorithm for clonal identification avoids
141 this type of bias, leading to the inference of the true tree and the true mutational
142 history (**Fig. 2C**).

143

144 Furthermore, the fact that different sets of samples obtained from the same
145 primary tumor can generate two distinct, and incorrect, evolutionary histories
146 (**Fig. 1B** and **Fig. 2B**) suggests that phylogenetic analysis of mutational profiles
147 from bulk tumor tissues can be less straightforward than previously thought.

148

149 *Relative timing of metastasis*

150 Another potential issue associated with the use of composite clones is
151 determining the evolutionary relationships between the primary tumor and distant
152 metastases. Following a similar approach to Zhao *et al.*¹⁹, consider now a patient
153 for which four distinct samples have been sequenced: a primary tumor sample
154 and three metastases (**Fig. 3A**). For simplicity, we assume that (i) there is no
155 contamination from healthy cells, (ii) only the primary tumor hosts several clones,
156 and (iii) somatic mutations accumulate linearly with time (i.e., following a
157 molecular clock). In this example, there are four true clones (A-D). Clone A
158 represents the ancestral lineage from which the other clones derived. Clone B,
159 which was never sampled/existed in the primary tumor, represents the first
160 metastasis (metastasis I), followed by migration of clone C (metastasis II) and
161 later of clone D (metastasis III) into three distinct anatomical regions (**Fig. 3B**,
162 right-panel).

163

164 By assuming that a single clone occurs (or dominates) in each sample, as in Zhao
165 *et al.*¹⁹, the primary tumor would be represented by a composite clone that never
166 existed (**Fig. 3C**, left-panel). In consequence, if we reconstruct a MP tree from
167 these data we will wrongly infer that metastasis II occurred before metastasis I –
168 because in this case the lineage leading to metastasis II diverges before the
169 lineage leading to metastasis I – and that mutations 4 and 5 evolved in parallel in

170 the primary tumor and in metastasis II (**Fig. 3C**, right-panel). Moreover, because
171 the composite clone for the primary tumor carries all mutations it is tempting to
172 conclude that it represents the youngest clone (perhaps resulting from a recent
173 selective sweep) when in fact is the oldest lineage. Conversely, if we use the
174 observed VAFs to deconvolute the clones present in each sample, despite clone
175 A not being identified by the clustering algorithm (**Fig. 3D**, left-panel), we will infer
176 a phylogenetic tree that accurately represents the evolutionary history of this
177 cancer (**Fig. 3D**, right-panel).

178

179

180 *Analysis of real data*

181 Since the examples above represent speculative scenarios, we reanalysed three
182 multiregional datasets in order to understand whether the use of mutational
183 profiles *versus* the use of inferred clones can also lead to different conclusions in
184 real scenarios. In the first study, Hao *et al.*¹⁶ investigated the spatial distribution
185 of ITH in esophageal squamous cell carcinoma. Using mutational profiles, the
186 authors reconstructed sample trees for several patients and found multiple cases
187 where mutations were “incompatible” with the inferred tree. Interestingly, these
188 are precisely those (parallel) mutations that appear more than once
189 (**Supplementary Fig.2A**). Conversely, when we inferred the clones present in
190 the samples and reconstructed their history, all parallel changes disappeared
191 (**Supplementary Fig.2B**). We argue that in fact the latter scenario seems much
192 more plausible.

193

194 In another study, Ling *et al.*¹⁸ relied on mutational profiles of 23 regional samples
195 to investigate the evolutionary dynamics of a hepatocellular carcinoma. Unlike
196 the original study, in which the spatial diversity patterns suggested seven major
197 mutational lineages with well-defined spatial boundaries (**Supplementary**
198 **Fig.3A**), a clonal analysis points instead to the presence of four clonal lineages
199 segregating at different frequencies across the regional samples with substantial
200 spatial overlap (**Supplementary Fig.3B**).

201

202 Finally, Gerlinger *et al.*¹⁴ explored the clonal architecture of clear cell renal
203 carcinoma by analysing the patterns of spatial ITH in multiple patients. Although

204 VAFs were in this case used to predict the clonal composition of each regional
205 sample, the identification of regional subclones was limited to those samples
206 showing strong visual evidence of multiple clonal populations (i.e., displaying
207 clusters of mutations with clearly distinct allele frequency patterns). As a
208 consequence, the full clonal architecture was not completely resolved, which in
209 turn may have compromised the derived evolutionary inferences. In case EV007,
210 for instance, clear signals of intraregional heterogeneity were only observed for
211 two samples (R3 and R9) and the inferred MP tree suggested five instances of
212 parallel evolution at the FAM110B, TSKU, TPRG1, NOP2 and BAP1 genes, the
213 latter being a tumor suppressor gene identified as a putative driver
214 (**Supplementary Fig.4A**). In contrast, a joint formal analysis of the VAFs of all
215 regional samples suggests an alternative evolutionary scenario, with three clonal
216 lineages showing an uneven distribution across the different subsections of the
217 tumor (**Supplementary Fig.4B**). Notably, the clonal tree implies a single parallel
218 mutation at the FAM110B gene.

219

220 **DISCUSSION**

221 We have shown that the use of absence/presence mutational profiles obtained
222 from bulk sequencing of tissue samples can compromise the study of tumor
223 evolution. Given the pervasiveness of ITH, the types of biases we have
224 demonstrated here - including wrong clonal histories, spurious parallel changes,
225 reversed timings of metastases and/or incorrect phylogeographic patterns - might
226 be commonplace suggesting that the interpretation of previous studies might
227 need to be reevaluated. Furthermore, as already demonstrated by Kostadinov *et*
228 *al.*²¹, the use of mutational profiles may also result in inaccurate branch length
229 estimates, leading to an overestimation of substitution rate heterogeneity among
230 samples that can be confounded with positive selection. Consequently, bulk
231 mutational profiles need to be interpreted with caution, as without complete
232 information of the clonal composition of each tumor different evolutionary
233 scenarios might fit the observed ITH patterns.

234

235 Fortunately, powerful statistical inferential methods are currently being developed
236 to characterize the clonal composition of bulk tumor samples, which generally
237 rely on sequencing-depth information and estimates of allele frequencies^{20,22-24}.

238 While the relative performance of these methods has not been yet thoroughly
239 benchmarked, it seems clear from our examples that they could be very helpful
240 in reducing the level of uncertainty of the evolutionary inference from tumor bulk
241 samples. In fact, not all multiregional tumor sequencing studies to date have
242 relied on bulk mutational profiles. A few have already based their evolutionary
243 inferences on clonal sequences estimated from the data (e.g., Gundem *et al.*⁷;
244 Yates *et al.*¹⁵; Ding *et al.*²⁵). Alternatively, single-cell sequencing data might soon
245 become the preferred type of data for the evolutionary analysis of tumors,
246 provided the technical limitations and the inherent sample bias arising from a
247 limited number of cells are solved^{26–28}.

248

249 Nevertheless, it is clear from our analyses that in multiregional tumor studies it is
250 important to distinguish “sample trees”, which depict the resemblance among
251 different regions of the tumor (or among temporal samples), from “clone trees”,
252 which depict the history of the genetic lineages inhabiting the tumor. In
253 evolutionary biology, these type of trees are analogous to “population/species
254 trees” and “gene trees”, respectively (e.g., Tajima²⁹, Pamilo & Nei³⁰; Page &
255 Charleston³¹ for a review). Gene trees are embedded inside population trees in
256 the same way as clonal lineages evolve along different tumor regions, although
257 tumor samples should be much more admixed than organismal population
258 samples.

259

260 Outside cancer genomics, potential biases resulting from the evolutionary
261 analysis of pooled individuals (“pool-sequencing”) have been already identified
262 and several corrections have been proposed for the estimation of allele
263 frequencies, diversity indices, SNP calling, population structure, tests of
264 neutrality or association tests from pool-seq data³². Some of these corrections
265 might be applicable in the cancer scenario.

266

267 In the future, complementary strategies combining clonal estimates derived from
268 bulk-sequencing data with single-cell information should provide a more precise
269 view of the clonal architecture of tumors, which could ultimately be used to
270 improve cancer prognosis and therapy.

271

272 **ACKNOWLEDGMENTS**

273 We would like to thank Andrés Pérez-Figueroa, Inigo Martincorena, Harald
274 Detering and Sara Rocha for their comments on earlier versions of the
275 manuscript. This work was supported by the European Research Council (ERC-
276 617457- PHYLOCANCER awarded to D.P.) and by the Ministry of Economy and
277 Competitiveness - MINECO (BFU2015-63774-P awarded to D.P.). T.P. was
278 supported by a PhD fellowship from the Galician Government (ED481A-
279 2015/083) and a PhD fellowship from the Spanish Government (FPU15/03709).

280

281 **AUTHOR CONTRIBUTIONS**

282 D.P. conceived the project and designed the analyses. D.P., J.M.A. and T.P.
283 performed the analyses. J.M.A. and D.P. wrote the manuscript.

284

285 **COMPETING FINANCIAL INTEREST**

286 The authors declare no competing financial interests.

287

288 **MATERIALS & CORRESPONDENCE:**

289 David Posada (dposada@uvigo.es)

290 Phylogenomics Lab, Edificio Torre CACTI, Campus Universitario, Universidad de
291 Vigo 36310 Vigo, Spain. (+34) 986 130050

292

293

294 **REFERENCES**

- 295 1. Burrell, R. A., McGranahan, N., Bartek, J. & Swanton, C. The causes and
296 consequences of genetic heterogeneity in cancer evolution. *Nature* **501**, 338–345
297 (2013).
- 298 2. Greaves, M., Mel, G. & Maley, C. C. Clonal evolution in cancer. *Nature* **481**, 306–
299 313 (2012).
- 300 3. Aparicio, S. & Caldas, C. The implications of clonal genome evolution for cancer
301 medicine. *N. Engl. J. Med.* **368**, 842–851 (2013).

- 302 4. Andor, N. *et al.* Pan-cancer analysis of the extent and consequences of intratumor
303 heterogeneity. *Nat. Med.* **22**, 105–113 (2016).
- 304 5. Nik-Zainal, S. *et al.* The life history of 21 breast cancers. *Cell* **149**, 994–1007
305 (2012).
- 306 6. Jiao, W., Vembu, S., Deshwar, A. G., Stein, L. & Morris, Q. Inferring clonal
307 evolution of tumors from single nucleotide somatic mutations. *BMC Bioinformatics*
308 **15**, 35 (2014).
- 309 7. Gundem, G. *et al.* The evolutionary history of lethal metastatic prostate cancer.
310 *Nature* **520**, 353–357 (2015).
- 311 8. Stephens, P. J. *et al.* The landscape of cancer genes and mutational processes in
312 breast cancer. *Nature* **486**, 400–404 (2012).
- 313 9. Nik-Zainal, S. *et al.* Mutational processes molding the genomes of 21 breast
314 cancers. *Cell* **149**, 979–993 (2012).
- 315 10. Sottoriva, A. *et al.* A Big Bang model of human colorectal tumor growth. *Nat.*
316 *Genet.* **47**, 209–216 (2015).
- 317 11. Williams, M. J., Benjamin, W., Barnes, C. P., Graham, T. A. & Andrea, S.
318 Identification of neutral tumor evolution across cancer types. *Nat. Genet.* **48**, 238–
319 244 (2016).
- 320 12. Gerlinger, M. *et al.* Intratumor Heterogeneity and Branched Evolution Revealed by
321 Multiregion Sequencing. *N. Engl. J. Med.* **366**, 883–892 (2012).
- 322 13. Zhang, J. *et al.* Intratumor heterogeneity in localized lung adenocarcinomas
323 delineated by multiregion sequencing. *Science* **346**, 256–259 (2014).
- 324 14. Gerlinger, M. *et al.* Genomic architecture and evolution of clear cell renal cell
325 carcinomas defined by multiregion sequencing. *Nat. Genet.* **46**, 225–233 (2014).
- 326 15. Yates, L. R. *et al.* Subclonal diversification of primary breast cancer revealed by
327 multiregion sequencing. *Nat. Med.* **21**, 751–759 (2015).
- 328 16. Hao, J.-J. *et al.* Spatial intratumoral heterogeneity and temporal clonal evolution in
329 esophageal squamous cell carcinoma. *Nat. Genet.* (2016). doi:10.1038/ng.3683

- 330 17. Beerenwinkel, N., Schwarz, R. F., Gerstung, M. & Markowetz, F. Cancer evolution:
331 mathematical models and computational inference. *Syst. Biol.* **64**, e1–25 (2015).
- 332 18. Ling, S. *et al.* Extremely high genetic diversity in a single tumor points to
333 prevalence of non-Darwinian cell evolution. *Proceedings of the National Academy*
334 *of Sciences* **112**, E6496–E6505 (2015).
- 335 19. Zhao, Z.-M. *et al.* Early and multiple origins of metastatic lineages within primary
336 tumors. *Proceedings of the National Academy of Sciences* **113**, 2140–2145
337 (2016).
- 338 20. Zare, H. *et al.* Inferring clonal composition from multiple sections of a breast
339 cancer. *PLoS Comput. Biol.* **10**, e1003703 (2014).
- 340 21. Kostadinov, R., Maley, C. C. & Kuhner, M. K. Bulk Genotyping of Biopsies Can
341 Create Spurious Evidence for Heterogeneity in Mutation Content. *PLoS Comput.*
342 *Biol.* **12**, e1004413 (2016).
- 343 22. Fischer, A., Vázquez-García, I., Illingworth, C. J. R. & Mustonen, V. High-definition
344 reconstruction of clonal composition in cancer. *Cell Rep.* **7**, 1740–1752 (2014).
- 345 23. Oesper, L., Mahmoody, A. & Raphael, B. J. THetA: inferring intra-tumor
346 heterogeneity from high-throughput DNA sequencing data. *Genome Biol.* **14**, R80
347 (2013).
- 348 24. Popic, V. *et al.* Fast and scalable inference of multi-sample cancer lineages.
349 *Genome Biol.* **16**, 91 (2015).
- 350 25. Ding, L. *et al.* Clonal evolution in relapsed acute myeloid leukaemia revealed by
351 whole-genome sequencing. *Nature* **481**, 506–510 (2012).
- 352 26. Gawad, C., Koh, W. & Quake, S. R. Single-cell genome sequencing: current state
353 of the science. *Nat. Rev. Genet.* **17**, 175–188 (2016).
- 354 27. Navin, N. E. Cancer genomics: one cell at a time. *Genome Biol.* **15**, (2014).
- 355 28. Navin, N. E. The first five years of single-cell cancer genomics and beyond.
356 *Genome Res.* **25**, 1499–1507 (2015).

- 357 29. Tajima, F. Evolutionary relationship of DNA sequences in finite populations.
358 *Genetics* **105**, 437–460 (1983).
- 359 30. Pamilo, P. & Nei, M. Relationships between gene trees and species trees. *Mol.*
360 *Biol. Evol.* **5**, 568–583 (1988).
- 361 31. Page, R. D. & Charleston, M. A. Trees within trees: phylogeny and historical
362 associations. *Trends Ecol. Evol.* **13**, 356–359 (1998).
- 363 32. Schlötterer, C., Tobler, R., Kofler, R. & Nolte, V. Sequencing pools of individuals -
364 mining genome-wide polymorphism data without big funding. *Nat. Rev. Genet.* **15**,
365 749–763 (2014).

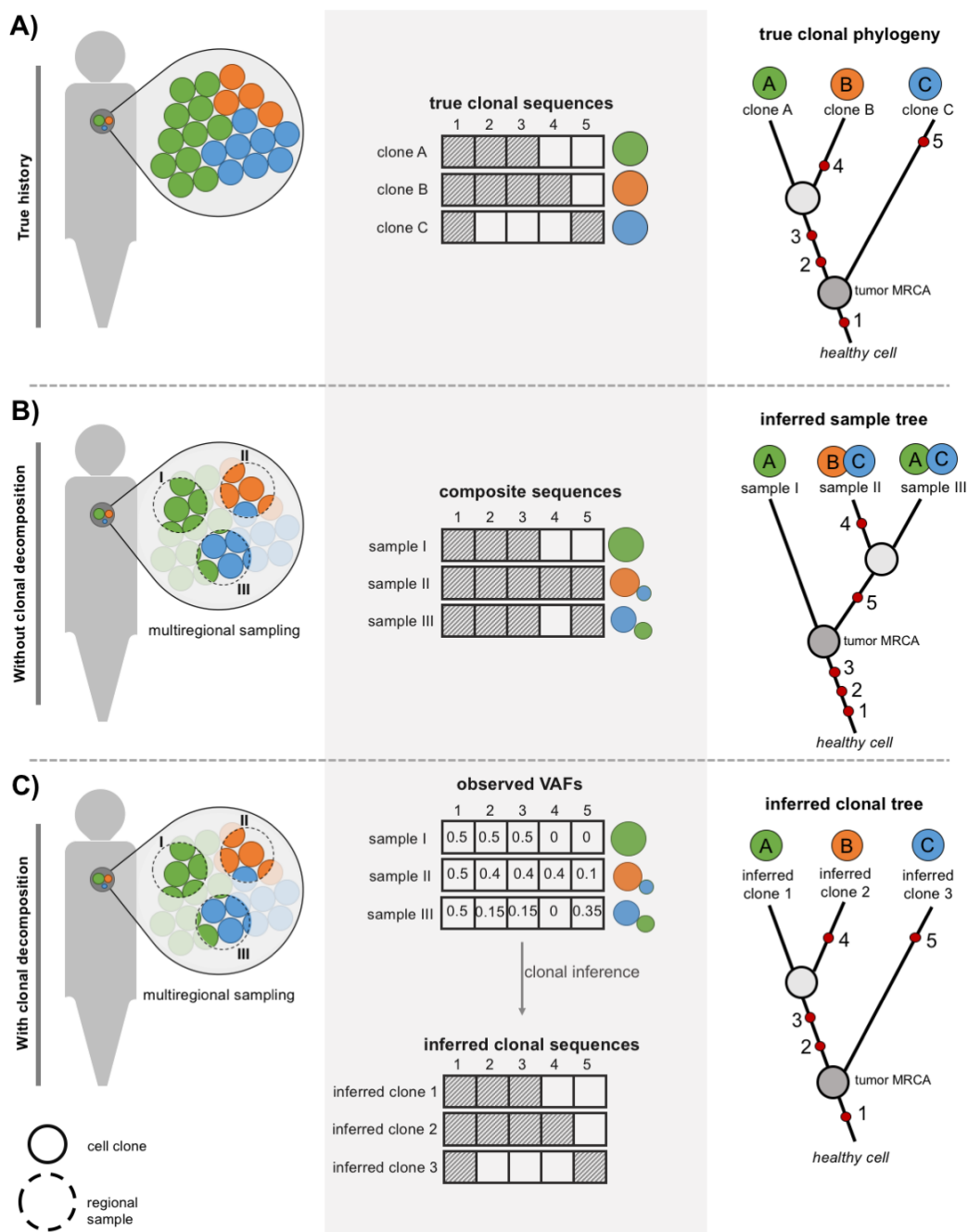
366

367

368

369

370



371

372

373

374

375

376

377

378

379

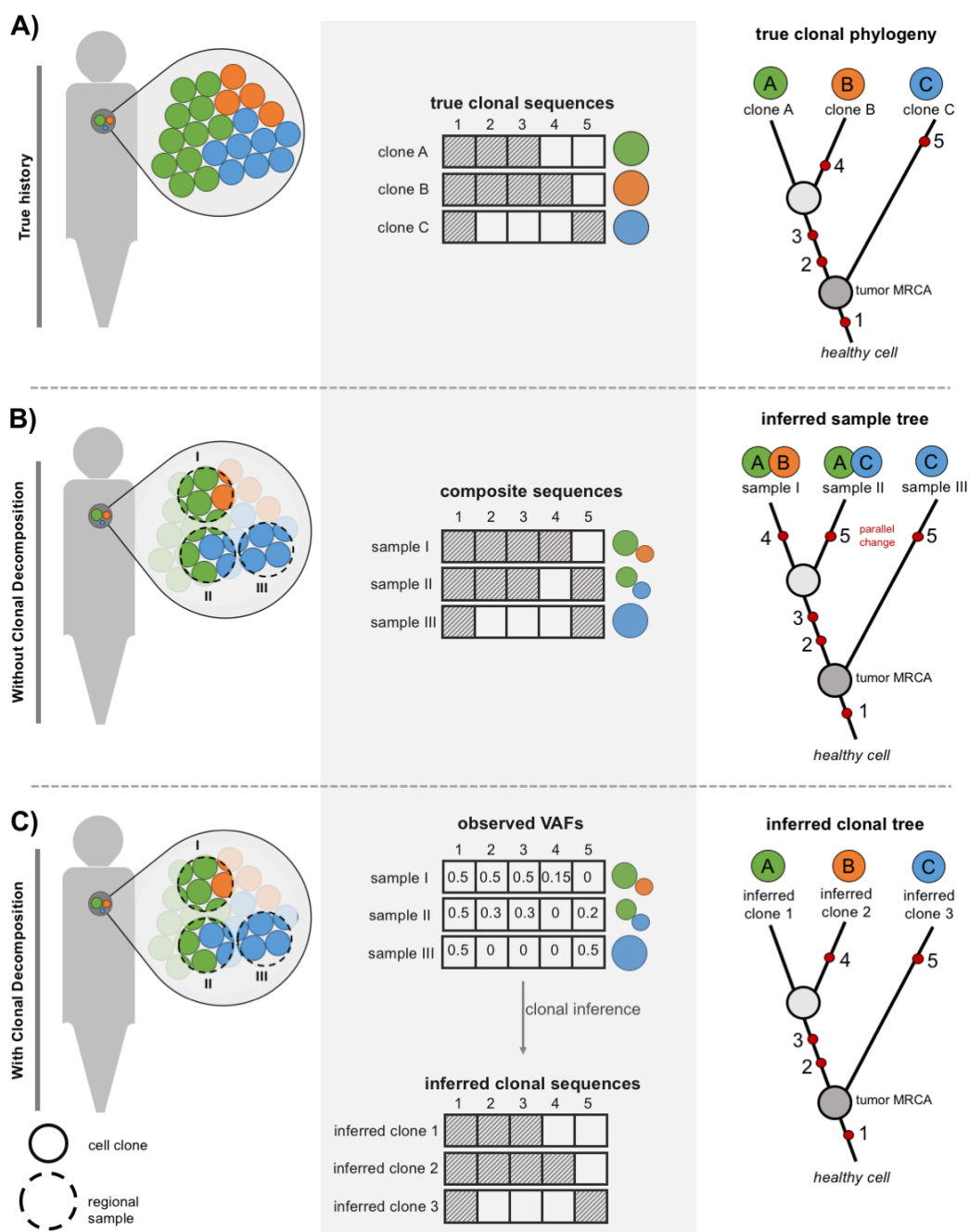
380

381

382

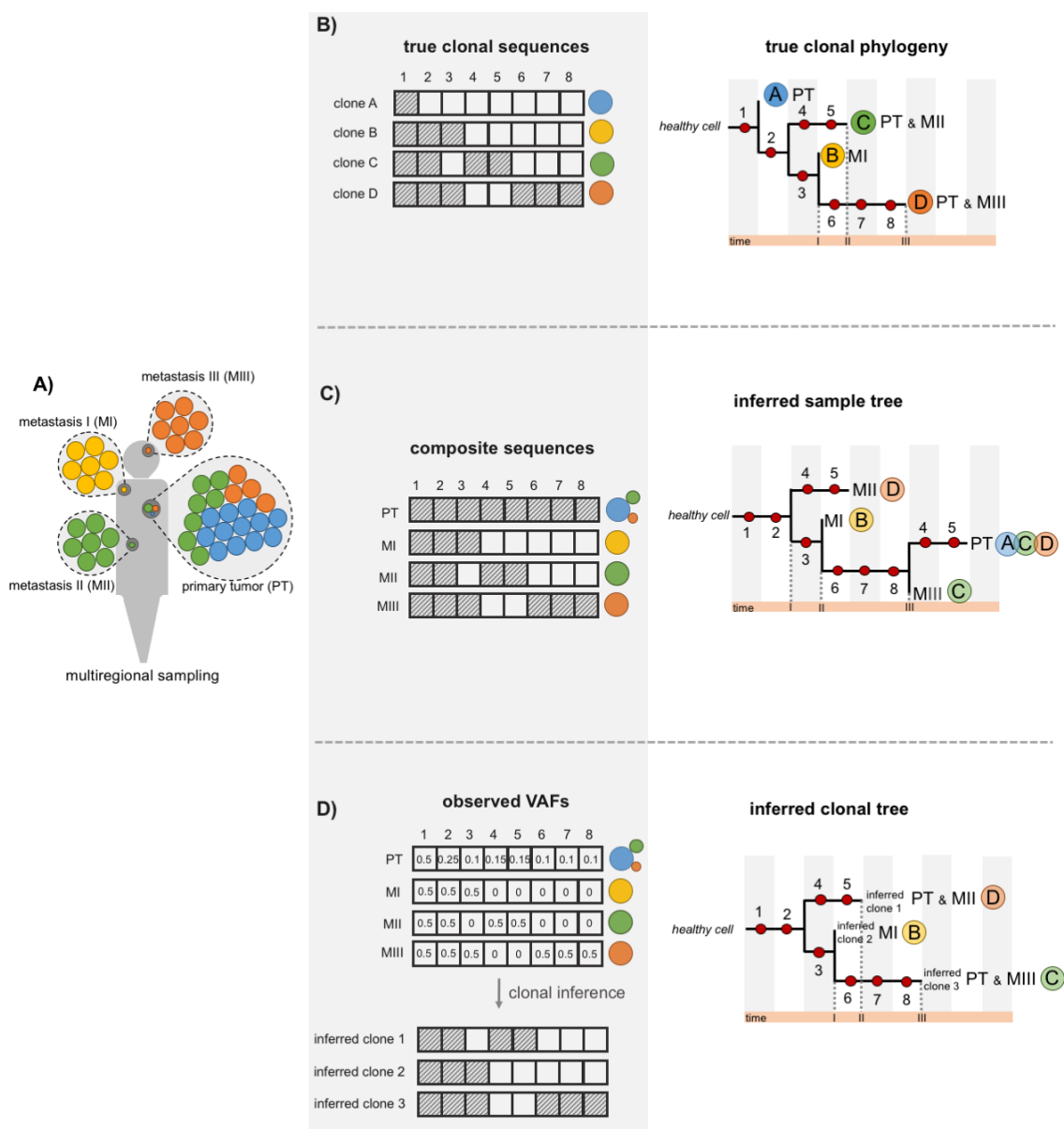
383

Figure 1. Phylogenetic analysis of bulk tumor samples (I). **A) Left-panel:** clonal composition of a hypothetical primary tumor. Colored circles represent the three clones present (A-C). **Mid-panel:** true clonal sequences for five different genomic sites, where the dashed square indicates a somatic mutation. **Right-panel:** true clonal history with red dots depicting the chronological order of mutations. Tumor most recent common ancestor (MRCA) highlighted as an internal node. **B) Left-panel:** bulk regional samples (I-III), with intermixed clones at different proportions. **Mid-panel:** composite sequences (presence/absence) inferred, dashed square indicates presence of mutation. **Right-panel:** inferred sample history using maximum parsimony. Red dots depict the inferred chronological order of mutations. **C) Left-panel:** bulk regional samples (I-III), with intermixed clones at different proportions. **Mid-panel:** variant allele frequency estimates for mutation at each sample, and inferred clonal sequences using the Clomial algorithm (see supplementary note for details). **Right-panel:** inferred clonal history using maximum parsimony. Red dots depict the inferred chronological order of mutations.



384

385 **Figure 2. Phylogenetic analysis of bulk tumor samples (II).** **A) Left-panel:** clonal composition of a
 386 hypothetical primary tumor. Colored circles represent the three clones present (A-C). **Mid-panel:** true clonal
 387 sequences for five different genomic sites, where the dashed square indicates a somatic mutation. **Right-**
 388 **panel:** true clonal history with red dots depicting the chronological order of mutations. Tumor most recent
 389 common ancestor (MRCA) highlighted as an internal node. **B) Left-panel:** bulk regional samples (I-III), with
 390 intermixed clones at different proportions. **Mid-panel:** composite sequences (presence/absence) inferred,
 391 dashed square indicates presence of mutation. **Right-panel:** inferred sample history using maximum
 392 parsimony. Red dots depicting the chronological order of mutations. **C) Left-panel:** bulk regional samples (I-
 393 III), with intermixed clones at different proportions. **Mid-panel:** variant allele frequency estimates for mutation
 394 at each sample, and inferred clonal sequences using the Clomial algorithm (but see supplementary note).
 395 **Right-panel:** inferred clonal history using maximum parsimony. Red dots depicting the chronological order
 396 of mutations.



397

398 **Figure 3. Incorrect chronological ordering of metastatic events using composite**
 399 **sequences.** **A)** Sampling scheme of geographically distinct tumor samples: one primary tumor
 400 and three metastatic sites. Colored circles represent the four cellular clones present (i.e., A, B, C
 401 and D). **B) Left-panel:** Clonal sequences based on genotype information from 8 somatic mutations
 402 - dashed square indicates presence of mutation. **Right-panel:** True clonal phylogenetic tree and
 403 geographical location of each clone. Chronological order of metastatic events depicted in the
 404 orange bar below the tree. **C) Left-panel:** Derived regional genotype sequences using
 405 presence/absence states. **Right-panel:** Inferred sample tree using maximum likelihood or
 406 maximum parsimony for the composite sequences. Inferred chronological order of metastatic
 407 events depicted in the orange bar below the regional tree. **D) Left-panel:** Allele frequency
 408 estimates of each mutation per regional sample, and inferred clonal sequences using Clomial
 409 algorithm (but see supplementary note). **Right-panel:** Phylogenetic tree drawn from the inferred
 410 clones (ICs) and inferred geographical location of each clone. Inferred chronological order of
 411 metastatic events depicted in the orange bar below the clonal tree.